NIH Public Access
Author Manuscript
Vaccine. Author manuscript; available in PMC 2009 March 28.

Published in final edited form as:
Vaccine. 2008 March 28; 26(15): 1863–1873.

Age-dependent tolerance to an endogenous tumor-associated antigen

Jennifer A. McWilliams[1], **Richard T. Sullivan**[1], **Kimberly R. Jordan**[1], **Rachel H. McMahan**[1], **Charles B. Kemmler**[1], **Marcia McDuffie**[2], and **Jill E. Slansky**[*,1]

1*Integrated Department of Immunology, University of Colorado, Denver*

2*Department of Microbiology, University of Virginia School of Medicine*

Abstract

Immunologic tolerance to endogenous antigens reduces antitumor responses. Gp70 is an endogenous tumor-associated antigen (TAA) of the BALB/c-derived colon carcinoma CT26. We found that expression of *gp70* mRNA is detectable in tissues of mice 8 months of age and older. We showed that expression of gp70 establishes immunologic tolerance and affects antitumor immunity in a similarly age-dependent manner using gp70-deficient mice. We found that tumors grew in all gp70-sufficient mice, while approximately half of gp70-deficient mice controlled tumor growth with endogenous T cell responses. Protection in gp70-deficient mice correlated with more robust gp70-specific CTL responses, and increased numbers and avidity of responding antigen-specific T cells after vaccination. We conclude that immunosurveillance may decline with age due to increased or de novo peripheral expression of endogenous TAAs.

Keywords

Tumor-associated antigen; immunologic tolerance; immunosurveillance

1. Introduction

Many factors decrease immunosurveillance of tumors by cytotoxic T lymphocytes (CTL) impairing effective antitumor responses [reviews [1-4]]. Tumor-associated macrophages, myeloid-derived suppressor cells, and regulatory T cells reduce effector functions of tumor-specific CTL. In addition, tumor cells secrete inhibitory cytokines and produce other factors associated with chronic inflammation that reduce antitumor responses. Finally, most tumor-associated antigens (TAAs) are derived from non-mutated self proteins, resulting in deletion of CTL with high avidity for TAAs. Thus, the T cells that may be most effective against tumors are deleted during negative selection in the thymus [5-7].

Experiments using transgenic mice expressing T cell receptor (TCR) genes and transfected TAAs have elucidated many of the obstacles that prevent the development and function of tumor-reactive T cells. The influence of antigen-specific tolerance varies depending on the number and source of T cells [8,9]. Examination of transferred cognate transgenic T cells into

Postal address: 1400 Jackson St, Denver CO 80206, Phone: (303) 398-1887, Fax: (303) 398-1396, Email: Jill.Slansky@UCHSC.edu.

Publisher's Disclaimer: This is a PDF file of an unedited manuscript that has been accepted for publication. As a service to our customers we are providing this early version of the manuscript. The manuscript will undergo copyediting, typesetting, and review of the resulting proof before it is published in its final citable form. Please note that during the production process errors may be discovered which could affect the content, and all legal disclaimers that apply to the journal pertain.

NIH-PA Author Manuscript
NIH-PA Author Manuscript
NIH-PA Author Manuscript

NIH-PA Author Manuscript

NIH-PA Author Manuscript

NIH-PA Author Manuscript

tumor-bearing hosts has determined the conditions for optimal effector function and may have general clinical applications [reviewed in [10]], but the function of a diverse T cell repertoire differs from that of a T cell clone [11]. In polyclonal systems, T cell function varies with the diversity of the repertoire, the avidity for antigen-presenting cells, and the precursor population size [12-14]. Thus, it is not clear that the rules established from experiments using monoclonal T cell systems with high affinity TCRs are applicable to polyclonal T cell repertoires. The role of the antigen in controlling the T cell response to tumors is also unclear. Many studies use transplantable tumors transfected with model antigens so that either transferred T cells or endogenous responses can be monitored [15,16]. Although the endogenous T cell responses to TAAs are typically weak and less amenable to experimentation [17] tumor model systems that employ the endogenous T cell repertoire and natural TAAs may provide more relevant results to guide the design of tumor immunotherapies.

T cell responses to TAAs encoded by endogenous retroviruses have been detected in both humans and mice [18,19]. Gamma-, or Type C, retroviruses are the most common retroviral elements in the human genome [20] and several examples have also been identified in mouse tumors [21]. In one example, the *gag* gene from Friend Leukemia Virus encodes an H-2D^{d}-restricted CTL target on the leukemia cell line, FBL-3 [22]. The ecotropic endogenous Murine Leukemia Virus (MuLV) also encodes TAAs from both gp70 (SU) and p15E (TM) proteins of the *env* gene. Both I-A^{b} and I-E^{b}-restricted peptides from MuLV have been identified in LB27.4 cells, a hybridoma of A20 lymphoma cells (H-2^{d}) and BW5147 cells (H-2^{b}) [23]. A CTL epitope p15E$_{604\text{-}611}$/H-2K^{b} was also identified from these cells [24] as well as from B16 tumor cells [25]. In CT26 tumor cells, a unique glycoslylated I-E^{d}-restricted epitope contributes to the CD4+ antitumor response [26], and CD8+ T cells respond to the dominant antigen gp70$_{423\text{-}431}$/H-2L^{d} (the AH1 antigen) [18]. *Gp70* mRNA and T cell responses to gp70-derived antigens are also detectable in other murine tumor cells and models including the 4T1 mammary carcinoma [27], A20 lymphoma [28], and B16 and S91 melanoma cells [18,29]. These findings suggest that the shared gp70 antigen is a bona fide TAA, since these epitopes are derived from a non-mutated self-antigen that is up-regulated during the transformation process. Thus, gp70 is an ideal antigen for the study of the importance of self tolerance in antitumor immune responses directed against TAAs.

To determine the role of gp70 expression in the T cell response to the CT26 transplantable tumor, we produced a gp70-deficient mouse. In young mice under 6 months of age, we found that gp70-deficient mice elicited more gp70-specific T cells that exhibited greater binding avidity than those elicited in gp70-sufficient mice. These T cell responses were associated with prevention of tumor growth in about half of the gp70-deficient mice. These results suggest that, in spite of the suppressive factors and heterogeneity of tumors that influence the quality of antitumor responses, successful antitumor CTL responses can be elicited in the absence of endogenous TAA expression in normal tissues. Furthermore, vaccination of gp70-sufficient mice over 8 months of age did not produce detectable TAA-specific T cells, although responses to a foreign antigen were readily detected. We also detected *gp70* mRNA expression in normal tissues of gp70-sufficient mice, particularly in mice older than 8 months. We propose that the age-related increase in expression of gp70 and subsequent T cell tolerance occur with other TAAs and cognate T cells. These results may explain the variable results observed in the clinic with immunotherapy directed against some TAAs and may suggest criteria for selection of some TAAs over others for more successful immunotherapy.

NIH-PA Author Manuscript

NIH-PA Author Manuscript

NIH-PA Author Manuscript

2. Materials and Methods

2.1 Generation of BALB.B6 env-/- (gp70-/-, gp70-deficient) congenic mice and littermate controls (gp70+/+, gp70-sufficient)

All animal experiments were performed in accordance with protocols approved by the Institutional Animal Care and Use Committee of National Jewish Medical and Research Center. CB6F1/Cr [(BALB/cAnNCr x C57BL/6NCr)$_{F1}$] male and BALB/cAnNCr female mice were purchased from the NCI-Frederick Animal Production Program, bred together, and the offspring were screened by PCR for heterozygosity surrounding the MuLV integration containing a functional gp70 gene at 28.71 Mb of Chr 5 in BALB/c mice using D5MIT387 and D5MIT148 (Chr 5, 28.7 and 32.3 Mb, respectively; NCBI, build m36). Mice were screened using 139 primer sets (Table 1) that flank simple sequence length polymorphisms (SSLPs) distinguishing the two parental strains. Most of the congenic mice used in these experiments were backcrossed 5 generations with the details of the breeding/selection scheme presented in Table 1. The mice used in Fig 3a were backcrossed 3 generations and Fig 5a were backcrossed 16 generations to BALB/c; after the fifth backcross, only D5MIT387 and D5MIT148 were used in the screening. We define young mice as 6 months of age and under, and middle-aged mice as 8 to 12 months of age.

2.2 PCR screening of genomic DNA

Genomic DNA from tail tissue was extracted after 16 h at 55°C in Lysis Buffer (500 mM KCl, 100 mM Tris pH 8.3, 15 mM $MgCl_2$, 4.5% NP-40, 4.5% Tween 20) and 0.2 mg/ml proteinase K. The resulting solution was cleared by centrifugation, and then extracted with equal volumes of phenol, phenol/chloroform, and chloroform. The DNA was ethanol precipitated and then dissolved overnight in water. The DNA concentration was adjusted to 125 ng/μl.

For the genome-wide screen of the N1 generation, PCR reactions were set up using a Multiprobe II Robotic Handling System (Parkard Bioscience Co.). Ten μl PCR reactions included PCR buffer, 5 nM each fluorescent primer (labeled with Fam, Hex, or Tet), 100 nM each nucleotide, 1 mM $MgCl_2$, 0.5 units Taq, and 20 ng DNA. Reactions were performed in a Hybrid TouchDown Thermal Cycler [94°C 1.5 min (first cycle only), 30 cycles of 94°C for 30 sec, 55°C for 1 min, and 72°C for 1 min]. Pools of up to eight loci distinguished by fluorescent tags and fragment sizes were combined and resolved by automated sequencers at the University of Maine sequencing facility. Samples were analyzed using Genotyper and Genescan software (Perkin-Elmer/Applied Biosystems).

For the screening of subsequent generations, 20 μl PCR reactions included 16 mM ammonium sulfate, 67 mM Tris pH 8.8, 0.05% TWEEN-20, 5 nM each primer, 200 nM each nucleotide, 1.5 mM $MgCl_2$, and 0.05 units Taq and 50 ng DNA. Reactions were performed in MJ Research Thermal Cycler [95°C 2 min (first cycle only), 30 cycles of 94°C for 15 sec, 57°C for 45 sec, and 72°C for 1 min]. Amplified DNA was resolved on 4% agarose gel and visualized with ethidium bromide.

2.3 Cells

CT26, CT26-GM, CT26-βgal-GM, MC57G-Ld, T2-Ld and the AH1-specific T cell clone were cultured as described [30].

2.4 RT-PCR

Tissues were homogenized and RNA was extracted using the Qiagen RNeasy Mini Kit, cDNAs were synthesized using the Qiagen QuantiTech Reverse Transcription Kit, and PCR was performed using Invitrogen Platinum PCR SuperMix as per the manufacturers' instructions. The products of the gp70-a forward [nucleotide (nt) 275, relative to the ATG] 5′

NIH-PA Author Manuscript

NIH-PA Author Manuscript

NIH-PA Author Manuscript

AGATCTCTGTATGTTGGCCCTCCA and gp70-a reverse (nt 462) 5′ TAAGTCTGTTCCAGGCCGTATTGC and gp70-b forward (nt 396) 5′ TCCAGAGATTGTGAGGAG and gp70-b reverse (nt 716) 5′ CCGGATAGTTAAGGAGTTGCA primers were within the region unique to this MuLV (nts 275-819, [31]). cDNA of mouse β–actin was amplified in all samples as a positive control: β–actin forward 5′ AGAGGGAAATCGTGCGTGAC and β–actin reverse 5′ CAATAGTGATGACCTGGCCGT. Reactions were performed in a MJ Research Thermal Cycler for the indicated number of cycles [94°C 2 min (first cycle only), 94°C for 30 sec, 58° C for 30 sec, and 72°C for 1 min] and resolved on 2% agarose gels.

2.5 Tumor growth assay, tumor protection assay, and peptide vaccines

For tumor growth assays, $5x10^4$ live CT26 tumor cells in 100 μl Hank's buffer (Cellgro, Mediatech, Inc.) were injected subcutaneously in the rear flank. Tumor growth was monitored over time by palpation of the injection site. Mice were sacrificed when the tumor reached 1 cm in any direction. Peptide vaccinations were performed as described [32]. Briefly, mice were injected with $1x10^5$ CT26 cells as above. Four and 6 days later, mice were injected with the indicated peptides and LANAC adjuvant [containing liposomes, CpG plasmid DNA, and 10 μg peptide as described [32,33]]. 14 days after tumor injection, when the tumors were still less than 1 cm in all directions, the tumors were removed and the infiltrating T cells were analyzed. For vaccination assays, 10^6 irradiated CT26-GM or CT26-βgal-GM cells were injected subcutaneously 16 or 14 and 7 days prior ex vivo examination or stimulation of splenocytes in culture as described [30]. Mice boosted with peptide received $5x10^6$ Sf9 cells infected with recombinant baculovirus encoding peptide/H-$2L^d$ [34].

2.6 Cytotoxicity assays

Prior to in vitro Chromium-release assays, $4x10^6$ splenocytes were combined with 10 U/ml IL-2 and 10 μg/ml AH1 peptide (SPSYVYHQF, Macromolecular Resources) and incubated in 24-well plates for 5 days at 37°C. Chromium-release assays were performed as described [30]. ^{51}Cr-labeled MC57G-Ld cells were incubated with the AH1 or MCMV pp89 peptide (YPHFMPTNL). In vivo killing assays were performed as described [34]. Briefly, splenocytes were loaded with the AH1 (CFSE-high) or βgal (CFSE-low, TPHPARIGL) peptide and injected intravenously into vaccinated mice. Percent specific lysis was determined as $1-[(\%\beta gal/\%AH1)_{unvaccinated} / (\%\beta gal/\%AH1)_{vaccinated}] \times 100$.

2.7 Antibodies and flow cytometric analyses

Splenocytes were stained ex vivo and after 7 days in culture with 10 U/ml IL-2 and 10 μg/ml AH1 peptide. Tumor-infiltrating lymphocytes were stained ex vivo. Antigen-specific T cells were identified using a live-gate, a dump-gate [included directly conjugated CD4 (GK1.5, ATCC), B220 (RA3.6B2, eBioscience), and MHC class II (M5/114.15.2, eBioscience) antibodies], H-$2L^d$ tetramers [32] and a CD8 antibody (53-6.7, eBioscience) as described [32]. CD3+ cells were stained with 2.C.11 antibody (eBiosciences). Background was decreased using an antibody against FcγR (2.4G2, ATCC). Quadrants were set using H-$2L^d$ tetramers loaded with βgal peptide. For V-beta analyses, cells were stained for 1 h with tetramer, CD8 antibody, and dump antibodies at 37°C, then without washing, cells were incubated on ice with the V-beta antibodies. The V-beta panel was purchased from BD Biosciences. All samples were analyzed using FlowJo software (Tree Star, Inc.).

NIH-PA Author Manuscript

NIH-PA Author Manuscript

NIH-PA Author Manuscript

3. Results

3.1 Derivation of a gp70-deficient mouse on the BALB/c background

Previous work showed that, despite the detection of T cell responses specific for the CT26 tumor, T cells cannot prevent tumor growth in normal BALB/c recipient mice [32]. Data from other investigators demonstrated that proteins from MuLV are expressed in BALB/c mice [35]. Therefore, we produced a gp70-deficient mouse strain to determine if the detectable, yet ineffective T cell responses to the CT26 tumor are limited by normal tolerance mechanisms or by antigen non-specific suppressive factors. Homology searching for the integration site of MuLV in BALB/c mice [36] matched with chromosome (Chr) 5 at 30.4 Mb. In C57BL/6 mice the virus matched with 124 Mb of Chr 8 of C57BL/6. The chromosomal locations are consistent with the mapping of the original genetic loci. Specifically, *env-1* and *env-3* of BALB/c and C57BL/6 were mapped to Chrs 5 and 8, respectively [37].

Taking advantage of the different integration sites of the proviruses, we deleted the BALB/c gp70 locus by marker-assisted replacement of the BALB/c Chr 5 integration site with that from the C57BL/6 background. After backcross of $(\text{BALB/c x C57BL/6})_{F1}$ mice to BALB/c, we selected offspring that were heterozygous for the BALB/c gp70 interval located between D5MIT387 (28.7 Mb) and D5MIT148 (32.3 Mb). Mice that were heterozygous at this interval were screened for BALB/c homozygosity at all other genetic markers, and those that contained the highest percentage of BALB/c alleles on all other chromosomes were used to breed the following generation. Since the C57BL/6 genome encodes the same MuLV on Chr 8, we selected for BALB/c homozygosity in this region during the second backcross. Based on microsatillite analyses, we estimated that we achieved greater than 99.5% homozygosity for BALB/c loci by the fifth backcross. Mice from this generation were intercrossed for the final congenic strain, which is homozygous for C57BL/6 alleles across an interval of less than 21 Mb around the site for viral integration in BALB/c mice (Table 1). The IL-6 gene is in the gp70 interval (30.34 Mb, Chr 5). However, there are no coding region sequence differences between the BALB/c and C57BL/6 alleles (Genbank accession numbers X54542 and AK150440). In addition, we did not detect different concentrations of IL-6 in serum after stimulation with poly I:C or in supernatants after 2 days of culture between the final congenic mouse strains (data not shown). We have not tested for polymorphisms between BALB/c and C57BL/6 for any of the other novel or known genes in this interval.

3.2 Gp70 mRNA is detectable in gp70-sufficient mice, but not gp70-deficient mice

To verify that our backcrossing strategy functionally deleted *gp70* expression from the congenic mice, we used an RT-PCR assay to assess mRNA expression. We used two primer sets within the probe identified by Chan et al. (gp70 a and gp70 b), which are near the 5′ region of the *gp70* transcript and are specific for this MuLV [31]. PCR analyses of cDNA produced from the CT26 tumor cell line resulted in bands of the expected sizes (Fig 1a). We confirmed that we indeed amplified the *gp70* sequence with both primer sets by DNA sequencing of the amplified fragments (data not shown). The sequence from the CT26 tumor was identical to NCBI sequence J01998 [with the changes predicted by Horowitz and Risser, [35]]. We detected *gp70* PCR products after 20 cycles of amplification from cDNA from the CT26 tumor cells. No *gp70* signal was obtained from the “no template” control reaction or control cells known not to express *gp70* transcripts, T2-Ld (human T2 cells transfected to express H-2L^d molecules, Fig 1b). *β-actin* cDNA was detected in all samples after 20 cycles of amplification, except in the absence of template.

To confirm that MuLV is not expressed in gp70-deficient mice, and to determine where it is expressed in gp70-sufficient mice, we surveyed RNA from tissues of mice that were at least 8 months of age using the assay described above (Figs 1c and d, Table 2). A time course from

NIH-PA Author Manuscript

NIH-PA Author Manuscript

NIH-PA Author Manuscript

previous experiments showed that MuLV replication and transcription takes place in the spleen of middle-aged mice treated with LPS, typically by 8 months of age, and continues into old age [38]. Consistent with these findings, we also detected *gp70* cDNA in tissues from gp70-sufficient mice over 8 months of age (Fig 1c). Expression of *gp70* was detected in normal colon from gp70-sufficient mice within 30 to 35 cycles of amplification. The amplified DNA sequence from the CT26 tumor and the normal colon tissue was identical (data not shown). The presence or absence of *gp70* mRNA from 7 other tissues is shown in Table 2. Of the six gp70-sufficient mice examined, only one was *gp70*-negative in all tissues, although β-actin was detected. This mouse was the same age and had been living in the same conditions as the others in the study. In addition, there was variability in the amounts of *gp70* mRNA expression in tissues; it was not detected in all samples of any one tissue. However, the PCR assay results from the RNA of individual tissues were reproducible. Asynchronous expression of *gp70* mRNA may be expected from an endogenous retrovirus that does not have a role in normal development, and for which the stimuli that induce viral expression may be environmental, but are unknown. Importantly, no *gp70* signal was detected in any of the samples from gp70-deficient mice.

3.3 The absence of gp70 mRNA expression correlates with improved endogenous anti-CT26 tumor responses

We next evaluated whether the absence of the *gp70* gene in the host results in enhanced antitumor immunity to CT26 tumor development (Fig 2). Gp70-sufficient and –deficient mice were injected with live CT26 cells and the injection site was monitored for tumor growth. Most of the gp70-sufficient mice developed tumors within 2 weeks, consistent with previous reports and our experience with this tumor [30,32]. However, only half of the gp70-deficient mice developed detectable tumors, confirming previous data [18] that the dominant T cell response is to the gp70 antigen and processing of the gp70 antigen in the tumor does not differ in gp70-sufficient or -deficient mice. As expected, depletion of CD4+ or CD8+ T cells resulted in increased tumor development in all gp70-deficient mice (data not shown). These results strongly suggest that tolerance mechanisms of the T cell repertoire decrease the response to endogenous TAA. However, not all of the gp70-deficient mice were tumor-free, suggesting that there are additional regulatory processes from immune cells and/or the tumor environment. Thus, as expected from experiments using foreign model tumor antigens [39,40], antitumor immunity is more robust when the immunizing antigen is foreign relative to self.

3.4 AH1-specific T cell function increases in the absence of the gp70 gene

Effective antitumor immunity correlates with detection of antigen-specific cytotoxic activity [41]. To determine if cells from the gp70-deficient mice kill tumor cells more effectively than cells from the gp70-sufficient mice, and to confirm that the AH1 epitope of gp70 is still recognized by CTL from gp70-deficient mice, we primed both gp70-sufficient and deficient mice with whole cell CT26 vaccines made by lethal irradiation of the tumor [18,42] and analyzed antigen-specific killing by T cells. One week after the second injection of vaccine, spleen cells from the immunized mice were placed in culture for 5 days with the AH1 peptide and then used in standard Chromium-release assays. As shown in Fig 3a, cells from the gp70-deficient mice lysed more CT26 cells than cells from the gp70-sufficient mice. To confirm that T cells indeed recognized the AH1 epitope from CT26 cells, MC57G-Ld cells incubated with peptide were used as targets. AH1-loaded targets were lysed in a dose-dependent manner, whereas the cells loaded with an irrelevant target from MCMV were not (Fig 3b).

To confirm that gp70-deficient mice elicit a more robust cytotoxic T cell response to the AH1 antigen than gp70-sufficient mice, and to determine whether the reduced tumor development correlated with increased CTL activity in the gp70-deficient mice, we performed in vivo killing assays (Fig 3c). Young mice were vaccinated with CT26-GM and then tested for antigen-

NIH-PA Author Manuscript

NIH-PA Author Manuscript

NIH-PA Author Manuscript

specific cytotoxic activity by injecting equal numbers of CFSE-high splenocytes incubated with the AH1 peptide and CFSE-low splenocytes incubated with the βgal peptide. As in the in vitro assay, significantly more AH1-loaded targets were killed in gp70-deficient than gp70-sufficent mice. The reduced functional CTL activity in the gp70-sufficient mice is another indication that gp70-sufficient animals exhibit T cell tolerance to the AH1 antigen.

3.5 The AH1-specific T cell repertoire changes in the absence of the gp70 gene

Since gp70 is a self protein in gp70-sufficient mice, immune tolerance, specifically negative selection of gp70-specific T cells, is likely responsible for the difference in antitumor immunity between the gp70-sufficient and -deficient mice (Fig 2). Negative selection may lead to decreased cytotoxic activity elicited by antigen-specific vaccines observed in gp70-sufficient mice (Fig 3), decreased avidity of the antigen-specific T cells, or differences in the V-beta usage of the responding T cells. We tested these possibilities by analyzing AH1-specific T cells from the gp70-sufficient and –deficient mice.

To determine if the cytotoxic response to the AH1 peptide in the gp70-deficient mice (Fig 3) is due to a higher frequency of T cells or T cells with improved lytic function, we characterized tumor-specific T cells infiltrating CT26 tumors (Fig 4a). Young gp70-sufficient and -deficient mice were injected with tumor cells and vaccinated with the AH1 peptide to boost the response. Then tumor-infiltrating lymphocytes (TIL) were analyzed for tetramer staining. There were 4 to 5-fold more CD8+ AH1-specific TIL in tumors from gp70-deficient mice. In addition, these T cells bound AH1-tetramer more intensely, indicating qualitative differences in the T cells (right panels, Figs 4a and 4b). Although tetramer intensity does not always correlate with the avidity of T cells [43], when the T cells express similar amounts of CD8 and TCR molecules, then correlations can be made [32,44]. TIL from gp70-sufficient and -deficient tumors express similar amounts of CD8 (Fig 4a) and TCR molecules (Fig 4b) suggesting that the T cells from the gp70-deficient mice are likely to bind antigen with higher avidity. To determine if antitumor immunity in the gp70-deficient mice is mediated by the same repertoire of T cells relative to gp70-sufficient mice, we examined the V-beta usage of T cells responding to the tumor using a panel of V-beta antibodies (Fig 4c). The response in the gp70-deficient mice was generally broader, consistent with the hypothesis that the AH1-specific T cell repertoire is subjected to more stringent negative selection in the gp70-sufficient mice as a result of self tolerance. These data suggest that both the quantity and quality of the T cell response is improved in the gp70-deficient mice.

3.6 Middle-aged gp70-sufficient mice do not generate TAA-specific T cells in response to a whole tumor cell vaccine

As described above, previous studies showed that MuLV proteins are not detectable in young mice but are induced in middle-age and subsequently remain detectable throughout the life of the mouse [38]. Consistent with these findings, we found *gp70* mRNA in peripheral tissues in mice over 8 months of age (Figure 1, Table 2). Next, we determined if antitumor immunity also changes in middle age due to increased antigen expression. We vaccinated young and middle-aged gp70-sufficient and –deficient mice with irradiated CT26 tumor cells engineered to express GM-CSF (CT26-GM), and analyzed the frequency of AH1-specific T cells ex vivo and after one week in culture. As shown in Fig 5a, these T cells were detected in gp70-deficient mice of both age groups and young gp70-sufficient mice, but not in middle-aged gp70-sufficient mice ex vivo. Since the frequency of these T cells was close to the level of detection ex vivo, we cultured the T cells for one week under conditions that expand AH1-specific T cells, and re-analyzed them. Similar to the ex vivo data, the frequency of AH1-specific T cells from gp70-deficient mice was higher than gp70-sufficient mice and AH1-specific T cells were not detected in middle-aged gp70-sufficient mice. To confirm that this reduced response in the middle-aged gp70-sufficient mice was unique to gp70 (AH1), we vaccinated the gp70-

NIH-PA Author Manuscript

NIH-PA Author Manuscript

NIH-PA Author Manuscript

sufficient mice with CT26 and CT26-βgal tumor cells engineered to express GM-CSF and then examined the relative frequency of AH1- and βgal-specific T cells respectively, ex vivo (Fig 5b). The frequency of AH1-specific T cells was reduced again in the middle-aged mice, but the βgal-specific T cells in the young and middle-aged gp70-sufficient mice were similar. These results suggest that there is not a defect in the general T cell response in the middle-aged gp70-sufficient mice, but that increased gp70 expression results in specific tolerance and/or deletion of AH1-specific T cells.

To demonstrate that *gp70* mRNA was selectively expressed in middle-aged gp70-sufficient mice, we performed the RT-PCR assays shown in Fig 1 on tissue samples from young and middle-aged mice (Fig 5c). Only one of 4 young mice showed *gp70* expression in the colon and thymus. In contrast, *gp70* cDNA was amplified in the colon and thymus of all 4 middle-aged mice analyzed. *Gp70* signal was not detected from liver cDNA, although *β-actin* cDNA was detectable. These results are consistent with deletion or tolerance of AH1-specific T cells due to antigen presentation in the thymus and periphery.

Finally, to determine if gp70 expression and reduced frequency of AH1-specific T cells in the middle-aged gp70-sufficient mice correlated with reduced tumor protection, we tested whether vaccinating these mice with irradiated CT26 tumor cells engineered to express GM-CSF protected these mice from tumor development (Fig 5d). Using a vaccination protocol that protects 100% of young BALB/c mice from tumors, we vaccinated middle-aged gp70-sufficient and –deficient mice, challenged the mice with tumor, and monitored tumor growth. Four of nine middle-aged gp70-sufficient mice developed tumors with a delayed time course. No gp70-deficient mice developed tumors (data not shown). These results suggest that the immunologic tolerance to the gp70-antigen observed in middle-aged mice reduced the tumor protection below that afforded to younger mice.

4. Discussion

Using congenic mice lacking the endogenous ecotropic MuLV that encodes the MHC class I and II immunodominant tumor antigens from the CT26 tumor, we showed that (1) endogenous T cells specific for a natural TAA successfully prevent tumor development and (2) changes in expression of TAAs may lead to changes in immunologic tolerance and the efficacy of corresponding immunotherapies. The absence of the genomic interval encoding gp70 resulted in an improved T cell response against the CT26 tumor which correlates with more functional, larger, higher avidity, and more diverse TAA-specific T cell responses (Figs 3 and 4). Antibody depletion of CD4+ or CD8+ T cells ablated the tumor protection in the gp70-deficient mice (data not shown), demonstrating this resistance to tumor growth was dependent upon induction of T cell-mediated functions. T cells that escaped negative selection in young gp70-sufficient mice (Fig 5) control tumor growth after vaccination. However, these T cells were not detectable in middle-aged mice (Fig 5a) likely due to peripheral and central tolerance initiated by gp70 expression in peripheral tissues, lymph nodes, and the thymus. Loss of T cell responses to tolerance induction by delayed expression of gp70 resulted in improved survival and growth of CT26 cells in vivo (Fig 5d).

Because young gp70-sufficient mice clearly allow expansion of fewer gp70-specific T cells than gp70-deficient animals (Fig 5a), we hypothesized that gp70 protein is expressed in the thymus in concentrations below the limits of detection of our PCR assay, leading to negative selection of high avidity, antigen-specific T cells, and reduced T cell diversity. AIRE, a transcription factor in the thymus that regulates transcription of peripheral tissue antigens, may be responsible for low levels of *gp70* transcription leading to negative selection of specific T cells (see [45] for review). However, some T cells escape negative selection and can be activated by antigen-specific immunotherapies such as irradiated whole cell vaccines secreting

NIH-PA Author Manuscript

NIH-PA Author Manuscript

NIH-PA Author Manuscript

GM-CSF [42] or mimotope vaccines [32]. During middle-age, control of gp70 protein expression is more widely detectable throughout lymphoid organs and peripheral tissues (Figs 1 and 5, Table 2), suggesting widespread loss of control over epigenetic repression mechanisms. The resulting expression of gp70 protein enhances effective control of the remaining gp70-specific T cells by normal tolerance mechanisms, possibly by peripheral deletion, resulting in decreased efficacy of antigen-specific immunotherapies.

As mentioned above, earlier research showed that this MuLV is expressed in LPS-treated splenocytes from BALB/c and C57BL/6 mice over 8 months of age ex vivo [38]. Although expression of MuLV is low in these strains relative to the AKR strain [46], we readily detected *gp70* expression in a number of tissues from middle-aged mice (Figs 1 and 5,Table 2). Furthermore, using an RT-PCR assay, we found *gp70* mRNA in middle-aged gp70-sufficient mice in all tissues examined except the uterus (Table 2) and liver (Fig 5c). We did not detect *gp70* expression in fetal tissues or tissues from one week-old mice (data not shown). Since gp70 does not function in normal tissue development and the signals that activate *gp70* transcription are unknown, this variability in tissue expression is not surprising. Our reports differ from other reports in the literature. Other investigators could not detect *gp70* mRNA in Northern blot analyses of normal colonic epithelium from C57BL/6 mice [47]. Nor was it detected by RT-PCR analyses of BALB/c epithelial cells from gastrointestinal organs, testes, thymic stroma, and bone marrow-derived thymic elements [18] or Northern blot analyses other tissues from adult, newborn, and fetal mice from C57BL/6 (testes, thymus, liver, kidney, and brain) [29]. These discrepancies may result from variations in the ages and strains of the analyzed mice as well as the different sensitivities of the assays.

The utility of human endogenous retroviruses (HERVs) as targets for immunotherapies for cancer or as cancer markers is becoming more intriguing as more HERVs are being discovered. One family of HERVs, HERV-K, comprises 30-50 different proviruses many of which are recognized by the immune system [19,48]. HERV-K expression, specifically HERV-K-mel, is low in normal tissues and increased in many tumors [19,49,50]. HERV-K-specific T cells have been detected in melanoma patients [19] and antibody responses are present in many patients with tumors [48]. These antigens, particularly if they are cancer-specific, may provide targets for T cell-based therapies. Since endogenous retroviruses do not provide vital functions to the tumor, tumor-specific expression and subsequent recognition of these TAAs by CTL may contribute to a local tumor environment that favors immunosurveillance. However, as shown here, these endogenous viruses may also be expressed in normal peripheral tissues. Thus, responses to targeted retroviral TAAs may lead to autoimmunity [51] or antigen-specific T cell tolerance. This range of possible responses to a protein with unknown regulation and with no necessary function to the cell may help to explain the variability in tumor-specific responses in experimental and clinical observations. Understanding when and where viral antigens are expressed is critical. New technologies are necessary to investigate these highly repetitive sequences. Thus, development of retroviral-based vaccines for the treatment of human cancers provides a promising therapeutic avenue with further basic research.

Acknowledgements

We thank Jonathan M. Horowitz for the discussions on MuLV, Brian Kotzin for advice and microsatellite primer sets, the University of Virginia Mouse Genetics Core facility, especially Shama Satinover, for help with design of the mapping strategy to generate the congenic strain as well as technical aspects of microsatellite analysis, and Sarah Rowland for help with tumor protection experiments. This work was supported by NCI CA109560 and a seed grant from the Colorado Cancer League to J.E.S. K.R.J., R.H.M., and C.B.K. were supported in part by the Cancer Research Institute Predoctoral Emphasis Pathway in Tumor Immunology Fellowship.

NIH-PA Author Manuscript

NIH-PA Author Manuscript

NIH-PA Author Manuscript

References

1. Drake CG, Jaffee E, Pardoll DM. Mechanisms of immune evasion by tumors. Advances in immunology 2006;90:51–81. [PubMed: 16730261]
2. Finn OJ. Cancer vaccines: between the idea and the reality. Nat Rev Immunol 2003 Aug;3(8):630–41. [PubMed: 12974478]
3. Sica A, Bronte V. Altered macrophage differentiation and immune dysfunction in tumor development. J Clin Invest 2007 May;117(5):1155–66. [PubMed: 17476345]
4. Gajewski TF. Failure at the effector phase: immune barriers at the level of the melanoma tumor microenvironment. Clin Cancer Res 2007 Sep 15;13(18):5256–61. [PubMed: 17875753]
5. McMahan RH, Slansky JE. Mobilizing the low-avidity T cell repertoire to kill tumors. Seminars in cancer biology 2007 Aug;17(4):317–29. [PubMed: 17651986]
6. Theobald M, Biggs J, Hernandez J, Lustgarten J, Labadie C, Sherman LA. Tolerance to p53 by A2.1-restricted cytotoxic T lymphocytes. J Exp Med 1997 Mar 3;185(5):833–41. [PubMed: 9120389]
7. Colella TA, Bullock TNJ, Russell LB, Mullins DW, Overwijk WW, Luckey CJ, et al. Self-tolerance to the murine homologue of a tyrosinase-derived melanoma antigen: implications for tumor immunotherapy. J Exp Med 2000 Apr 3;191(7):1221–32. [PubMed: 10748239]
8. Nguyen LT, Elford AR, Murakami K, Garza KM, Schoenberger SP, Odermatt B, et al. Tumor growth enhances cross-presentation leading to limited T cell activation without tolerance. J Exp Med 2002 Feb 18;195(4):423–35. [PubMed: 11854356]
9. Wall EM, Milne K, Martin ML, Watson PH, Theiss P, Nelson BH. Spontaneous mammary tumors differ widely in their inherent sensitivity to adoptively transferred T cells. Cancer Res 2007 Jul 1;67 (13):6442–50. [PubMed: 17616705]
10. Gattinoni L, Powell DJ Jr, Rosenberg SA, Restifo NP. Adoptive immunotherapy for cancer: building on success. Nat Rev Immunol 2006 May;6(5):383–93. [PubMed: 16622476]
11. Kuchroo VK, Anderson AC, Waldner H, Munder M, Bettelli E, Nicholson LB. T cell response in experimental autoimmune encephalomyelitis (EAE): role of self and cross-reactive antigens in shaping, tuning, and regulating the autopathogenic T cell repertoire. Annu Rev Immunol 2002;20:101–23. [PubMed: 11861599]
12. Marzo AL, Klonowski KD, Le Bon A, Borrow P, Tough DF, Lefrancois L. Initial T cell frequency dictates memory CD8+ T cell lineage commitment. Nat Immunol 2005 Aug;6(8):793–9. [PubMed: 16025119]
13. Foulds KE, Shen H. Clonal competition inhibits the proliferation and differentiation of adoptively transferred TCR transgenic CD4 T cells in response to infection. J Immunol 2006 Mar 1;176(5): 3037–43. [PubMed: 16493062]
14. Ford ML, Koehn BH, Wagener ME, Jiang W, Gangappa S, Pearson TC, et al. Antigen-specific precursor frequency impacts T cell proliferation, differentiation, and requirement for costimulation. J Exp Med 2007 Feb 19;204(2):299–309. [PubMed: 17261633]
15. Cordaro TA, de Visser KE, Tirion FH, Graus YM, Haanen JB, Kioussis D, et al. Tumor size at the time of adoptive transfer determines whether tumor rejection occurs. Eur J Immunol 2000 May;30 (5):1297–307. [PubMed: 10820375]
16. Kedl RM, Jordan M, Potter T, Kappler J, Marrack P, Dow S. CD40 stimulation accelerates deletion of tumor-specific CD8(+) T cells in the absence of tumor-antigen vaccination. Proc Natl Acad Sci USA 2001 Sep 11;98(19):10811–6. [PubMed: 11526222]
17. Drake CG, Doody AD, Mihalyo MA, Huang CT, Kelleher E, Ravi S, et al. Androgen ablation mitigates tolerance to a prostate/prostate cancer-restricted antigen. Cancer Cell 2005 Mar;7(3):239–49. [PubMed: 15766662]
18. Huang AYC, Gulden PH, Woods AS, Thomas MC, Tong CD, Wang W, et al. The immunodominant major histocompatibility class I-restricted antigen of a murine colon tumor derives from an endogenous retroviral gene product. Proc Natl Acad Sci USA 1996;93:9730–5. [PubMed: 8790399]
19. Schiavetti F, Thonnard J, Colau D, Boon T, Coulie PG. A human endogenous retroviral sequence encoding an antigen recognized on melanoma by cytolytic T lymphocytes. Cancer Res 2002 Oct 1;62 (19):5510–6. [PubMed: 12359761]

NIH-PA Author Manuscript

NIH-PA Author Manuscript

NIH-PA Author Manuscript

20. Consortium. IHGS. Initial sequencing and comparative analysis of the mouse genome. Nature 2002 Dec 5;420(6915):520–62. [PubMed: 12466850]
21. Kershaw MH, Hsu C, Mondesire W, Parker LL, Wang G, Overwijk WW, et al. Immunization against endogenous retroviral tumor-associated antigens. Cancer Res 2001 Nov 1;61(21):7920–4. [PubMed: 11691813]
22. Chen W, Qin H, Chesebro B, Cheever MA. Identification of a gag-encoded cytotoxic T-lymphocyte epitope from FBL-3 leukemia shared by Friend, Moloney, and Rauscher murine leukemia virus-induced tumors. J Virol 1996 Nov;70(11):7773–82. [PubMed: 8892898]
23. Rudensky AY, Preston-Hurlburt P, Hong SC, Barlow A, Janeway CA Jr. Sequence analysis of peptides bound to MHC class II molecules. Nature 1991 Oct 17;353(6345):622–7. [PubMed: 1656276]
24. White HD, Roeder DA, Green WR. An immunodominant Kb-restricted peptide from the p15E transmembrane protein of endogenous ecotropic murine leukemia virus (MuLV) AKR623 that restores susceptibility of a tumor line to anti-AKR/Gross MuLV cytotoxic T lymphocytes. J Virol 1994 Feb;68(2):897–904. [PubMed: 8289392]
25. Yang JC, Perry-Lalley D. The envelope protein of an endogenous murine retrovirus is a tumor-associated T-cell antigen for multiple murine tumors. J Immunother 2000;23(2):177–83. [PubMed: 10746543]
26. Golgher D, Korangy F, Gao B, Gorski K, Jaffee E, Edidin M, et al. An immunodominant MHC class II-restricted tumor antigen is conformation dependent and binds to the endoplasmic reticulum chaperone, calreticulin. J Immunol 2001;167(1):147–55. [PubMed: 11418643]
27. Luznik L, Slansky JE, Jalla S, Borrello I, Levitsky HI, Pardoll DM, et al. Successful therapy of metastatic cancer using tumor vaccines in mixed allogeneic bone marrow chimeras. Blood 2003;101:1645–52. [PubMed: 12406877]
28. Ali S, Ahmad M, Lynam J, Rees RC, Brown N. Trafficking of tumor peptide-specific cytotoxic T lymphocytes into the tumor microcirculation. Int J Cancer 2004 Jun 10;110(2):239–44. [PubMed: 15069688]
29. Hayashi H, Matsubara H, Yokota T, Kuwabara I, Kanno M, Koseki H, et al. Molecular cloning and characterization of the gene encoding mouse melanoma antigen by cDNA library transfection. J Immunol 1992 Aug 15;149(4):1223–9. [PubMed: 1380036]
30. Slansky JE, Rattis FM, Boyd LF, Fahmy T, Jaffee EM, Schneck JP, et al. Enhanced antigen-specific antitumor immunity with altered peptide ligands that stabilize the MHC-peptide-TCR complex. Immunity 2000;13(4):529–38. [PubMed: 11070171]
31. Chan HW, Bryan T, Moore JL, Staal SP, Rowe WP, Martin MA. Identification of ecotropic proviral sequences in inbred mouse strains with a cloned subgenomic DNA fragment. Proc Natl Acad Sci USA 1980 Oct;77(10):5779–83. [PubMed: 6255465]
32. McMahan RH, McWilliams JA, Jordan KR, Dow SW, Wilson DB, Slansky JE. Relating MHC-Peptide-TCR affinity to immunogenicity for the rational design of tumor vaccines. J Clin Invest 2006;116(9):2543–51. [PubMed: 16932807]
33. Dow SW, Elmslie RE, Willson AP, Roche L, Gorman C, Potter TA. In vivo tumor transfection with superantigen plus cytokine genes induces tumor regression and prolongs survival in dogs with malignant melanoma. J Clin Invest 1998 Jun 1;101(11):2406–14. [PubMed: 9616212]
34. Jordan KR, McMahan RH, Oh JZ, Pipeling MR, Pardoll DM, Kedl RM, et al. Baculovirus-infected insect cells expressing peptide-MHC complexes elicit protective antitumor immunity. J Immunol. 2007In Press
35. Horowitz JM, Risser R. Molecular and biological characterization of the endogenous ecotropic provirus of BALB/c mice. J Virol 1985 Dec;56(3):798–806. [PubMed: 2999434]
36. Horowitz JM, Holland GD, King SR, Risser R. Germ line integration of a murine leukemia provirus into a retroviruslike sequence. J Virol 1987 Mar;61(3):701–7. [PubMed: 3027396]
37. Risser R, Horowitz JM, McCubrey J. Endogenous mouse leukemia viruses. Annu Rev Genet 1983;17:85–121. [PubMed: 6320713]
38. McCubrey J, Risser R. Genetic interactions in the spontaneous production of endogenous murine leukemia virus in low leukemic mouse strains. J Exp Med 1982 Aug 1;156(2):337–49. [PubMed: 6284854]

NIH-PA Author Manuscript

NIH-PA Author Manuscript

NIH-PA Author Manuscript

39. Morgan DJ, Kreuwel HTC, Fleck S, Levitsky HI, Pardoll DM, Sherman LA. Activation of low avidity CTL specific for a self epitope results in tumor rejection but not autoimmunity. J Immunol 1998;160:643–51. [PubMed: 9551898]
40. Kedl RM, Rees WA, Hildeman DA, Schaefer B, Mitchell T, Kappler J, et al. T cells compete for access to antigen-bearing antigen-presenting cells. J Exp Med 2000;192(8):1105–14. [PubMed: 11034600]
41. Rubio V, Stuge TB, Singh N, Betts MR, Weber JS, Roederer M, et al. Ex vivo identification, isolation and analysis of tumor-cytolytic T cells. Nat Med 2003 Nov;9(11):1377–82. [PubMed: 14528297]
42. Dranoff G, Jaffee E, Lazenby A, Golumbek P, Levitsky H, Brose K, et al. Vaccination with irradiated tumor cells engineered to secrete murine granulocyte-macrophage colony-stimulating factor stimulates potent, specific, and long-lasting anti-tumor immunity. Proc Natl Acad Sci USA 1993;90:3539–43. [PubMed: 8097319]
43. Derby MA, Wang J, Margulies DH, Berzofsky JA. Two intermediate-avidity cytotoxic T lymphocyte clones with a disparity between functional avidity and MHC tetramer staining. Int Immunol 2001;13 (6):817–24. [PubMed: 11369710]
44. Crawford F, Kozono H, White J, Marrack P, Kappler J. Detection of antigen-specific T cells with multivalent soluble class II MHC covalent peptide complexes. Immunity 1998;8(6):675–82. [PubMed: 9655481]
45. Mathis D, Benoist C. A decade of AIRE. Nat Rev Immunol 2007 Aug;7(8):645–50. [PubMed: 17641664]
46. Freed EO, Risser R. The role of envelope glycoprotein processing in murine leukemia virus infection. J Virol 1987 Sep;61(9):2852–6. [PubMed: 3039173]
47. Hampton TA, Conry RM, Khazaeli MB, Shaw DR, Curiel DT, LoBuglio AF, et al. SEREX analysis for tumor antigen identification in a mouse model of adenocarcinoma. Cancer gene therapy 2000 Mar;7(3):446–55. [PubMed: 10766351]
48. Boller K, Janssen O, Schuldes H, Tonjes RR, Kurth R. Characterization of the antibody response specific for the human endogenous retrovirus HTDV/HERV-K. J Virol 1997 Jun;71(6):4581–8. [PubMed: 9151852]
49. Wang-Johanning F, Liu J, Rycaj K, Huang M, Tsai K, Rosen DG, et al. Expression of multiple human endogenous retrovirus surface envelope proteins in ovarian cancer. Int J Cancer 2007 Jan 1;120(1): 81–90. [PubMed: 17013901]
50. Schmitz-Winnenthal FH, Galindo-Escobedo LV, Rimoldi D, Geng W, Romero P, Koch M, et al. Potential target antigens for immunotherapy in human pancreatic cancer. Cancer letters 2007 Jul 18;252(2):290–8. [PubMed: 17320278]
51. Conrad B, Weissmahr RN, Böni J, Arcari R, Schüpbach J, Mach B. A human endogenous retroviral superantigen as candidate autoimmune gene in type I diabetes. Cell 1997 Jul 25;90(2):303–13. [PubMed: 9244304]

NIH-PA Author Manuscript
NIH-PA Author Manuscript
NIH-PA Author Manuscript

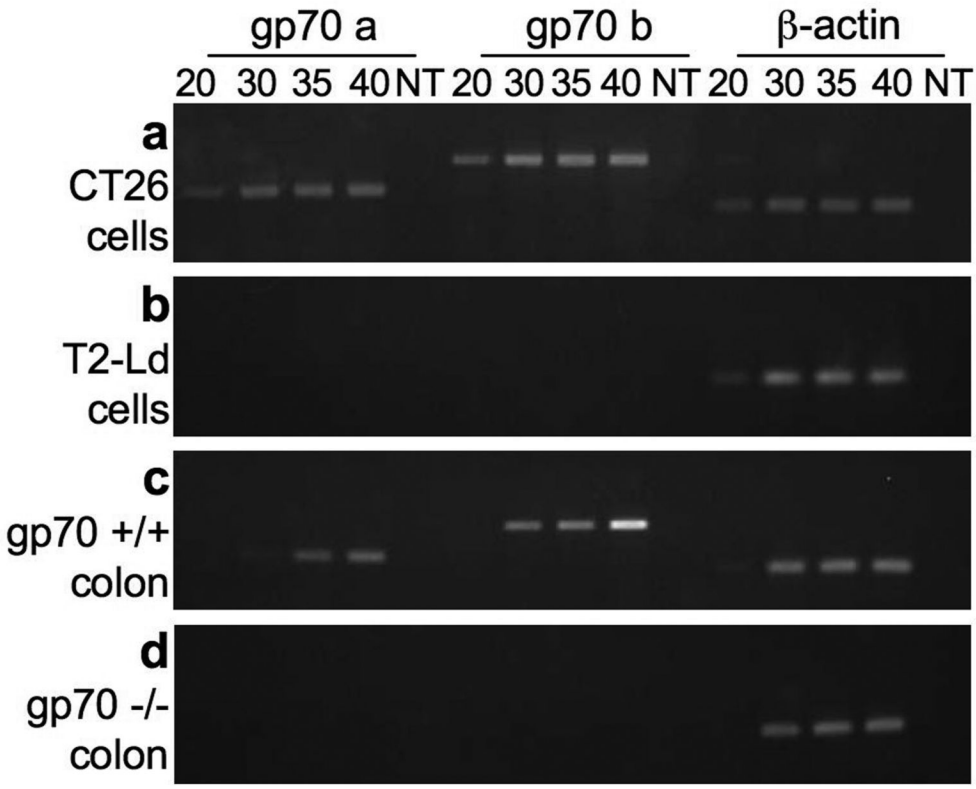

Fig 1. *Gp70* expression is detectable in CT26 tumor cells and in colon tissues from gp70-sufficient mice

mRNA was extracted from CT26 tumor cells (A), T2-Ld cells (B), and from the colons of gp70-sufficient (C), and gp70-deficient mice (D) (>8 months old). cDNA was produced and used in semi-quantitative RT-PCR reactions. Amplification was terminated at 20, 30, 35, and 40 cycles, and the DNA products were resolved on 2% agarose gels. *Gp70* and *β-actin* cDNAs were assayed. NT, no-template was assayed to monitor contaminants.

NIH-PA Author Manuscript

NIH-PA Author Manuscript

NIH-PA Author Manuscript

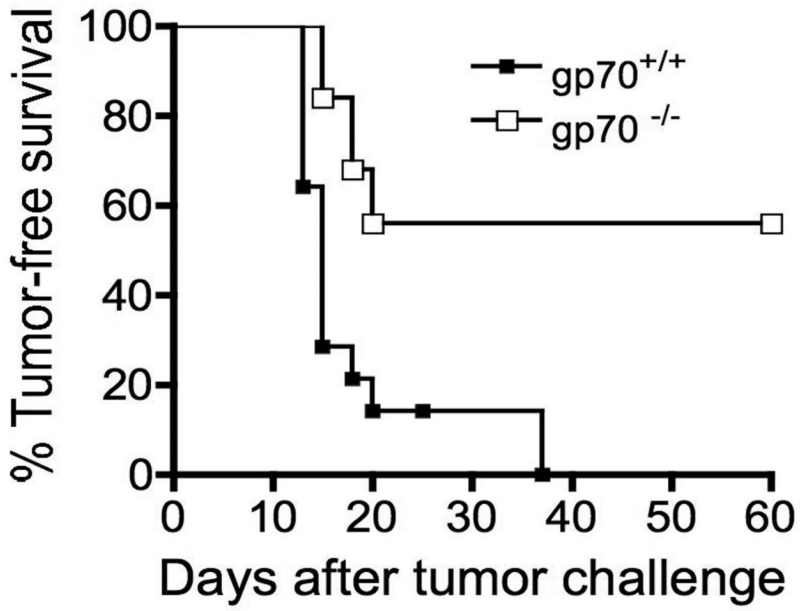

Fig 2. Approximately half of gp70-deficient mice are protected from CT26 tumor growth

Young (less than 4 months of age) gp70-deficient (n=14) and -sufficient (n=25) mice were injected with $5x10^4$ CT26 tumor cells and tumor growth was monitored for 60 days by palpation of the injection site. The two groups are significantly different ($p<0.0001$) as determined by the log rank test.

NIH-PA Author Manuscript

NIH-PA Author Manuscript

NIH-PA Author Manuscript

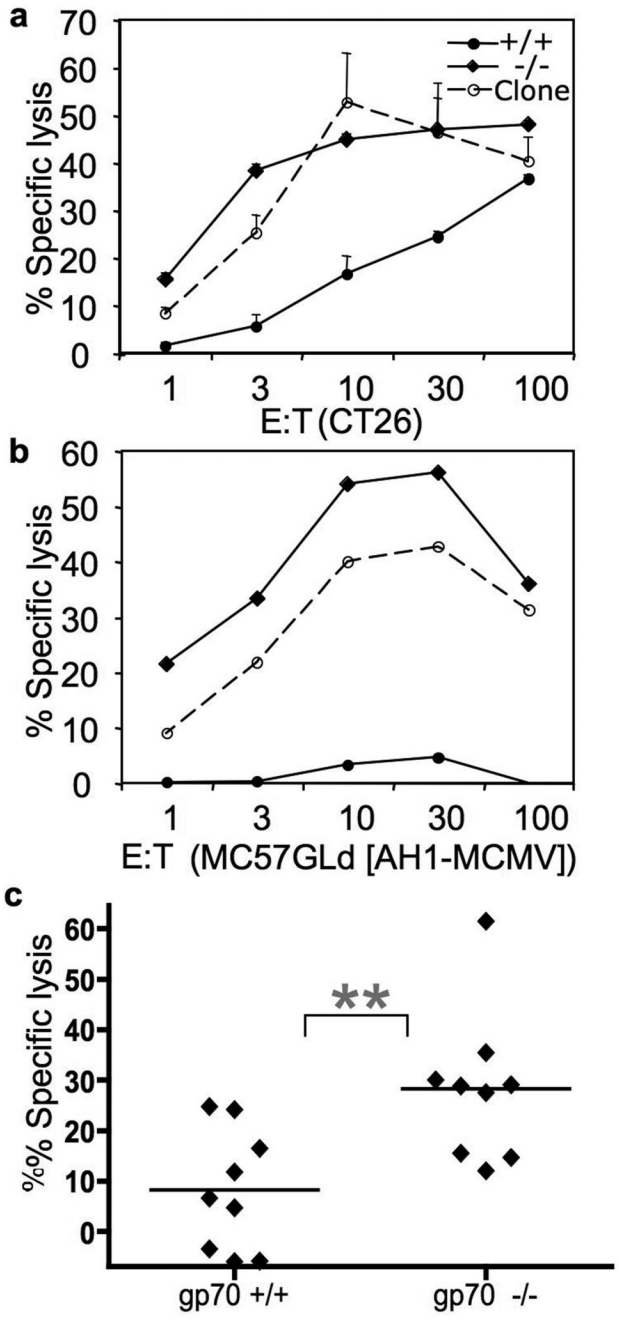

Fig 3. Gp70-deficient mice mediate more antigen-specific cytotoxic activity than gp70-sufficient mice in vitro and in vivo

^{51}Cr-labeled CT26 (A) and peptide-loaded MC57G-Ld (B) cells were combined with increasing numbers of the CT-T cell clone [dashed lines, [30]] or splenocytes from young (less than 4-months old) congenic mice backcrossed 3 generations, then intercrossed: gp70-deficient (diamonds), and gp70-sufficient mice (circles). B. Percent lysis of MC57G-Ld cells incubated with the AH1 peptide minus the MCMV peptide is shown. Percent lysis was calculated after 4 hours at 37°. The negative values are due to more chromium release from the MCMV-loaded targets relative to the AH1-loaded targets. A representative assay is shown; assays were performed in triplicate. C. Gp70-sufficient and -deficient mice that were less than 6-months

old, were vaccinated twice, one week apart with irradiated CT26-GM cells. Two million CSFE-labeled splenocytes, half incubated with the AH1 peptide and half with the βgal peptide, were injected and detected by flow cytometric analyses of the host spleen 24 h later. The bar represents the mean of the % specific lysis. The negative values in the gp70+/+ group are from mice that had more CFSE-low (βgal) cells than CFSE-high (AH1) cells, indicating that killing of AH1-loaded targets in this experiment was not detected. The 2 groups are significantly different (p=0.0061) as determined by a two-tailed unpaired t test.

NIH-PA Author Manuscript
NIH-PA Author Manuscript
NIH-PA Author Manuscript

NIH-PA Author Manuscript

NIH-PA Author Manuscript

NIH-PA Author Manuscript

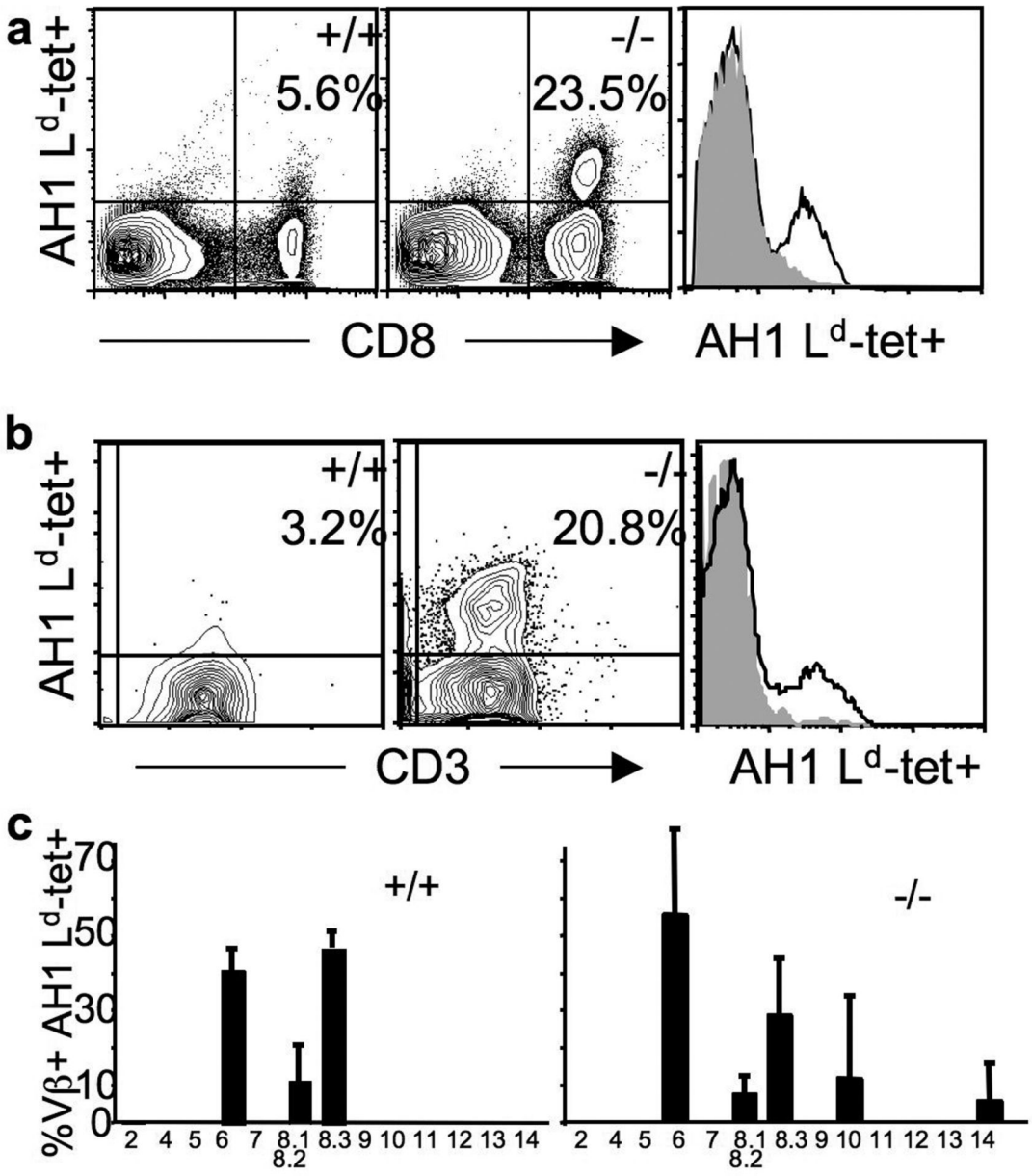

Fig 4. TAA-deficient mice generate a larger, more diverse, higher avidity TAA-specific T cell repertoire than TAA-sufficient mice

A. Young (less than 4-months of age) gp70-sufficient (+/+) and –deficient (-/-) mice were injected with live CT26 tumor cells and then 4 and 6 days later, were injected with AH1 peptide in adjuvant [32]. TIL were extracted and stained on day 14. The relative avidity of T cells was extrapolated from the mean fluorescence intensity (MFI) of tetramer on a Mo-Flo flow cytometer (DakoCytomation Inc.). The relative tetramer staining of the CD8+ cells is shown in the histogram on the right: MFI of CD8+ tet+ cells is 58 for the gp70+/+ mouse (grey filled), and 72 for the gp70-/- mouse (black line). The MFI of CD8 staining of the tet+ cells was 904 for TIL from the gp70-sufficient and 766 from the –deficient mouse. The data are representative of 4 experiments. B. Mice were treated as in A and data were collected on a Cyan flow cytometer (DakoCytomation Inc.). Live events gated on CD8+ cells are shown. The relative MFI of tetramer staining of the CD3+ cells is shown in the histogram on the right: MFI of CD8+ CD3

NIH-PA Author Manuscript

NIH-PA Author Manuscript

NIH-PA Author Manuscript

+ tet+ cells is 27.6 for the gp70+/+ mouse and 41.3 for the gp70-/- mouse. The MFI of CD3 staining of the tet+ cells was 36.9 for TIL from the gp70-sufficient and 30 from the –deficient mouse. The data are representative of 3 experiments. C. TIL from mice treated as in A were gated on L^d-tet/AH1+ CD8+ (y-axis) and costained with a panel of TCR V-beta antibodies (x-axis) from two mice. The y-axis scale is the same on both graphs.

NIH-PA Author Manuscript
NIH-PA Author Manuscript
NIH-PA Author Manuscript

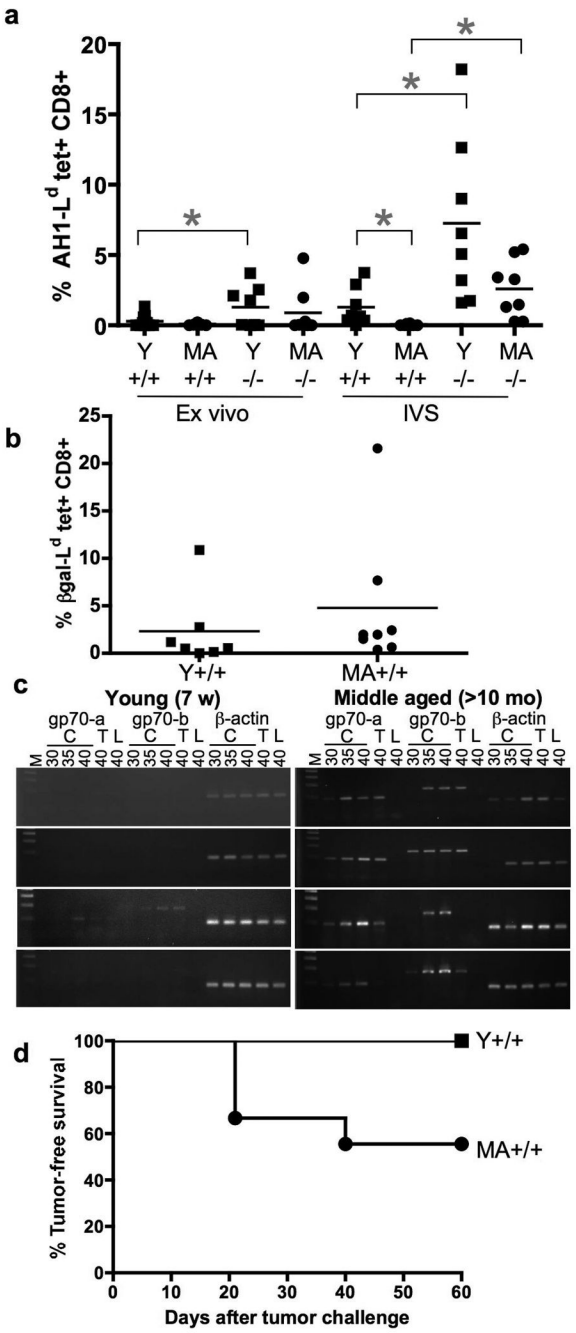

Fig 5. *Gp70* mRNA expression correlates with deletion of AH1-specific T cells detectable by tetramer staining

A. Young (Y, <7-weeks old) and middle-aged (MA, >8-months old) gp70-sufficient (+/+) and –deficient (-/-) mice were vaccinated with irradiated CT26 tumor cells engineered to express GM-CSF two times, one week apart. Splenocytes were stained with AH1 peptide-loaded tetramer and anti-CD8 antibody either ex vivo or after one week in culture. The percentage of AH1-specific T cells ex vivo in Y gp70-sufficient and –deficient mice is significantly different using an unpaired two-tailed t test (p=0.0453). The difference continues to be significant after one week in culture (p=0.0132), as is Y vs. MA gp70-sufficient (p=0.0199) and MA gp70-sufficient vs. gp70 deficient (p=0.0035). B. Splenocytes from mice vaccinated as in A, but with

NIH-PA Author Manuscript

NIH-PA Author Manuscript

NIH-PA Author Manuscript

CT26-βgal-GM were stained ex vivo with the H-2L^d tetramer loaded with the βgal peptide. The percentage of βgal-specific T cells in the Y and MA gp70-sufficient mice is the same (p=0.4999). C. Tissue from colon (C), thymus (T), and liver (L) was dissected from the young and middle-aged mice used in A, and PCR reactions were performed as described in Fig 1 and Table 2 for 30, 35, and 40 cycles. D. Young (squares, n=11) and middle-aged (circles, n=9) gp70-sufficient mice were injected with irradiated CT26-GM as in A, then one week after the last injection, were challenged and monitored as in Fig 2. The 2 groups are significantly different (p=0.0151) as determined by the log rank test.

NIH-PA Author Manuscript NIH-PA Author Manuscript NIH-PA Author Manuscript

Table 1

Simple sequence length polymorphisms used to generate BALB.B6 *env*-/- (gp70-deficient, -/-) and BALB.B6 *env*+/+ (gp70-sufficient, +/+) mice

A map of informative microsatellite polymorphisms was obtained from the Mouse Genetics Core at the University of Virginia. The chromosomal location of the genetic markers and the chromosome lengths were updated using the NCBI m36 consensus build of the C57BL/6 genome, August 2007 (www.ensembl.org/Mus_musculus/). "0" indicates that the band amplified by PCR was the size predicted from a homozygous BALB/c template, "1" indicates two products matching those from a heterozygous (BALB/c X C57BL/6)F_1 template.

			N1	N2	N3	N4	N5	N5
			M	M	M	F	M	F
chr/size	MB	mouse #/marker	19	7	10	132	2	4
1 197 MB	20	D1Mit3	0					
	33	D1Mit70		0				
	77	D1Mit132	0	0				
	88	D1Mit81	0					
	160	D1Mit33	1	0				
	180	D1Mit165	1	0				
	186	D1Mit291	1	0				
	190	D1Mit223	1	0				
	193	D1Mit209	1	0				
	195	D1Mit293	1	0				
	196	D1Mit155	1	0				
2 182 MB	3	D2Mit175		1	0			
	4	D2Mit1	1	1	0			
	28	D2Mit365	0	0				
	72	D2Mit11			0			
	86	D2Mit14		0	0			
	106	D2Mit214	0	0				
	128	D2Mit304	0					
	153	D2Mit285	0					
	173	D2Mit113	0					
3 160 MB	8	D3Mit221	0	0				
	53	D3Mit67	0	0				
	67	D3Mit241		0				
	91	D3Mit29	0					
	112	D3Mit106	0	0				
	148	D3Mit45	0	0				
4 152 MB	9	D4Mit264	0					
	26	D4Mit2	0	0				
	67	D4Mit178	0	0				
	91	D4Mit15	0	0				
	93	D4Mit166	0					
	99	D4Mit58	0	0				
	119	D4Mit334	0					
	136	D4Mit251	1	0	0			
	141	D4Mit32	1	0				
	149	D4Mit127	1	0				
5 152 MB	5	D5Mit346	1	0	0			
	15	D5Mit103		0	0			
	28	D5Mit386	1	1	1	1		
	28.7	D5Mit387			1	1	1	1
	30.4	MuLV						

NIH-PA Author Manuscript
NIH-PA Author Manuscript
NIH-PA Author Manuscript

			N1	N2	N3	N4	N5	N5
			M	M	M	F	M	F
chr/size	MB	mouse #/marker	19	7	10	132	2	4
	32.3	D5Mit148	1	1	1	1	1	1
	36	D5Mit352				0	0	0
	38	D5Mit13	1	1	1	0		
	65	D5Mit197	0	0				
	75	D5Mit201	0	0	0			
	109	D5Mit240	0					
	138	D5Mit98	0	0				
	149	D5Mit287	0	0				
	4	D6Mit86	1	0				
	15	D6Mit1	0	0				
	30	D6Mit159	0	0	0			
6	45	D6Mit223	0	0				
150 MB	53	D6Mit184	0					
	84	D6Mit8	0	0				
	104	D6Mit36	0	0				
	147	D6Mit373	0					
	4	D7Mit340	0					
	27	D7Mit77	0	0				
	35	D7Mit78	1	1	0			
7	51	D7Mit82		1	0			
145 MB	60	D7Mit249		1	0			
	128	D7Mit105	1		0			
	136	D7Mit109	0	0				
	144	D7Mit15	0					
	5	D8Mit155	0	0				
	37	D8Mit191	1					
	37	D8Mit190		0				
8	93	D8Mit107	1	0				
132 MB	114	D8Mit166	1	0				
	127	D8Mit49	1	0				
	130	D8Mit93	1					
	32	D9Mit90	0					
	34	D9Mit297		1				
	37	D9Mit247	1	1	0			
	44	D9Mit129	1					
9	69	D9Mit289	1		0			
124 MB	86	D9Mit11		1	0			
	101	D9Mit182	0	0				
	119	D9Mit82		0				
	121	D9Mit151	1					
	21	D10Mit2	0	0				
10	47	D10Mit194	0	0				
130 MB	66	D10Mit15	0					
	122	D10Mit35	0					
	3	D11Mit1			0			
	7	D11Mit71	1	1	0			
	20	D11Mit80			0			
11	45	D11Mit236	1					
122 MB	71	D11Mit320	1	1	0			
	80	D11Mit8		0				
	110	D11Mit100		0				

Vaccine. Author manuscript; available in PMC 2009 March 28.

NIH-PA Author Manuscript
NIH-PA Author Manuscript
NIH-PA Author Manuscript

			N1	N2	N3	N4	N5	N5
			M	M	M	F	M	F
chr/size	MB	mouse #/marker	19	7	10	132	2	4
	113	D11Mit168	1	0	0			
12 121 MB	11	D12Mit182	0					
	31	D12Mit136	0					
	71	D12Mit34	0					
	82	D12Mit5	0					
	103	D12Mit7	0					
	114	D12Mit19	0					
13 121 MB	20	D13Mit16	0					
	51	D13Mit221	0					
	77	D13Mit99		0				
	110	D13Mit148		0				
	113	D13Mit53	1	0				
	117	D13Mit151	0					
14 124 MB	14	D14Mit48	0					
	46	D14Mit60	0	0				
	61	D14Mit37		0				
	93	D14Mit194	0	0				
	104	D14Mit197	0	0				
	105	D14Mit170	0	0				
15 104 MB	13	D15Mit265		1	1	0		
	58	D15Mit121				0		
	65	D15Mit63	1	1	1	0		
	87	D15Mit159			1	1	0	0
16 98 MB	6	D16Mit55	0					
	36	D16Mit4	0	0				
	66	D16Mit139	0					
	93	D16Mit51	1					
	98	D16Mit106		0				
17 95 MB	25	D17Mit46		0				
	31	D17Mit175	1					
	34	D17Mit28		0				
	52	D17Mit139	1	0				
	57	D17Mit20		0				
	74	D17Mit39	1					
	90	D17Mit221	0					
18 91 MB	6	D18Mit64	0					
	30	D18Mit233	0	0				
	56	D18Mit123	0					
	85	D18Mit213	0					
19 61 MB	5	D19Mit59	0					
	25	D19Mit40	1					
	39	D19Mit19		0				
	47	D19Mit10	1	0				
	60	D19Mit71	1	0				
	61	D19Mit6		0				
20 165 MB	7	DXMit55	1	0	0			
	102	DXMit64	0					
	160	DXMit135	0	0				

NIH-PA Author Manuscript

NIH-PA Author Manuscript

NIH-PA Author Manuscript

Table 2

Gp70 mRNA is expressed in tissues of middle-aged gp70-sufficient mice [§]

Controls[†]	**gp70**[*]	**β-actin**	**gp70**[*]	**β-actin**
CT26 cells	+	+	+	+
T2-Ld cells	-	+	-	+
Normal tissues[§]	gp70+/+		gp70-/-	
Colon	5/6	6/6	0/6	6/6
Mesenteric lymph nodes	3/6	6/6	0/6	6/6
Thymus	2/6	6/6	0/6	6/6
Kidney	1/6	6/6	0/6	6/6
Spleen	1/6	6/6	0/6	6/6
Testis	2/3	3/3	0/4	4/4
Uterus	0/3	3/3	0/2	2/2

[§] Tissues were obtained from mice 8-mo or older

[†] Each experiment included cDNA from these control cells, and each PCR reaction was programmed for 40 cycles

[*] Gp70-a primers were used.